DR1. SUPPLEMENTAL METHODS

Experimental System Setup

Bacterial Enrichments

A consortium of acidophilic IOB was enriched from samples of fine-grained iron oxyhydroxide precipitates collected from Rio Tinto near Berrocal, Huelva, Spain (Shuster et al., 2014). These enrichments were obtained by inoculating 0.5 mL of the sample into 4 mL modified media defined by Silverman and Lundgren (1959) with 0.5 mL of 33.3 g/100 mL $FeSO_4 \cdot 7H_2O$ and pH adjusted to 2.3 using 2 M sulfuric acid. Six enrichments were incubated at room temperature (RT; ca. 22˚C) for three weeks in Fisherbrand® 13 × 100 mm borosilicate glass test tubes with plastic push caps to maintain aerobic conditions. One of the replicate enrichments was used for a cell count using the Most Probable Number (MPN) statistical method described by Cochran (1950). For the experimental system, five test tubes, each containing 1.2×10^5 MPN bacteria were added to the quartz sand. Note that the occurrence of mm-scale iron oxides minerals produced within the enrichment tubes possessed bacterial cells resulting in a slight underestimation of the iron-oxidizing bacterial population.

A sample of filamentous cyanobacteria with associated heterotrophs was obtained from a wetland near Atlin, British Columbia, Canada and enriched as a bacterial stock (Power et al., 2007). For this study, fresh cyanobacterial enrichments were obtained by inoculating 10 mL of the stock into 90 ml modified BG-11 medium (Rippka et al., 1979) incubated at RT in the presence of natural light for three months. After three months incubation, the cyanobacteria-dominated enrichment was stirred and agitated to evenly disperse the biofilms in solution for addition to the experimental system. Triplicate, 20 mL aliquots were collected on separate 0.45 µm pore-size filters and rinsed with distilled, deionized water. The filtrates were air-dried at RT

for 24 hours to determine the approximate dry weight of solid material including cyanobacteria, associated aerobic heterotrophs and carbonate minerals precipitates (500 mg) occurring in a 20 mL aliquot.

A consortium, enriching for SRB, was enrichment from samples collected from a borehole 3.2 km below land surface in the Driefontein gold mine, Witwatersrand Basin, Republic of South Africa (Moser et al., 2003; Lengke and Southam, 2006) in the modified medium defined by Postgate (1984). For the experimental system, SRB enrichments were grown by inoculating 1 mL aliquots of the SRB consortium into 12 mL of Postgate medium in screw-cap borosilicate glass tubes and incubated at RT for three weeks. The population of SRB was determined using scanning electron microscopy (SEM) of a filtered enrichment corresponding to ca. 1 pL (50 μm × 10 μm with a depth of view equaling approx. 2 μm). Bacterial counts from SEM micrographs estimated 4.5×10^8 cells/mL after three weeks of incubation; 1.2×10^{10} bacteria from this enrichment were added to the quartz sand to ensure that an active population of SRB was present.

Inductively Coupled Plasma-Atomic Emission Spectroscopy

A 10 mL fluid aliquot was sampled at two-week intervals and filtered twice using a 0.1 μm pore-size filter to remove any solid material. The pH of the filtered aliquots was measured using a Denver Instrument Basic pH Meter with an electrode calibrated to pH 7 and 10 reference standards using potassium biphthalate buffer at RT and margin of error was ± 0.04 units. The filtered aliquots were acidified with concentrated nitric acid (70%) and analyzed for soluble Au using a Perkin-Elmer Optima 3300-DV ICP-AES.

Scanning Electron Microscopy-Energy Dispersive Spectroscopy Analysis

Sampled Au grains were fixed using 2%$_{(aq)}$ glutaraldehyde for 24 h, dehydrated in a sequential 25, 50, 75 and 3 × 100% aqueous-ethanol series and dried using a Tousimis Research Corporation Samdri-PVT-3B critical point drier. Each sample was then mounted on a separate aluminum stub using 12 mm carbon adhesive tabs. A Denton Vacuum Desk II sputter coater was used to deposit a 5 nm thick osmium coating to prevent charging effects during SEM analysis. A LEO Zeiss 1540XB Field Emission Gun-Scanning Electron Microscope (FEG-SEM) operating at 3 kV and 10 kV accelerating voltage was used for imaging each sample in secondary and backscatter mode, respectively. Qualitative elemental analysis was determined using an Oxford Instruments' INCAx-sight Energy Dispersive Spectrometer (EDS). The same FEG-SEM was equipped with a Focused Ion Beam (FIB) that was used to mill various trough cross-sections 25 µm - 30 µm wide and 10 µm - 15 µm deep on the outer surface of cylindrical grains.

Transmission Electron Microscopy-Energy Dispersive Spectroscopy Analysis

Biofilms were fixed using 2%$_{(aq)}$ glutaraldehyde for 2 hours, enrobed in 2%$_{(wt/vol)}$ noble agar, dehydrated in a 25, 50, 75 and 3 × 100% aqueous-acetone series and embedded in Epon plastic. The embedded biofilms were cut to 70 nm ultrathin sections using a Reichert-Jung Ultracut E ultramicrotome and collected on Formvar-carbon coated, 200-square mesh copper grids. Ten-microliter aliquots of the experimental system fluid phase were prepared as whole mounts. All samples were imaged using a Phillips CM-10 TEM operating at 80 kV and equipped with an Energy Dispersive Spectrometer (EDS) X-ray microanalysis system.

REFERENCES

Cochran, W.G., 1950, Estimation of bacterial densities by means of the "Most Probable Number": Biometrics, v. 6, p. 105-116.

Lengke, M.F. and Southam, G., 2006, The bioaccumulation of gold by thiosulfate-reducing bacteria cultured in the presence of gold-thiosulfate complex: Geochimica et Cosmochimica Acta, v. 70, p. 3646-3661.

Moser, D.P., Onstott, J.K., Fredrickson, F.K., Brockman, F.J., Balkwill, D.L., Drake, G.R., Pfiffner, S., White, D.C., Takai, K., Pratt, L.M., Fong, J., Sherwood-Lollar, B., Slater, G., Phelps, T.J., Spoelstra, N., DeFlaun, M., Southam, G., Welty, A.T., Baker, B.J. and Hoek, J., 2003, Temporal shifts in the geochemistry and microbial community structure of an ultradeep mine borehole following isolaton: Geomicrobiology Journal, v. 20, p. 517-548.

Postgate, J.R., 1984, The sulfate-reducing bacteria. 2nd edition. Cambridge Press. 32.

Power, I.M., Wilson, S.A., Thom, J.M., Dipple, G.M. and Southam, G., 2007, Biological induced mineralization of dypingite by cyanobacteria from an alkaline wetland near Atlin, British Columbia, Canada: Geochemical Transaction, v. 8, p. 13.

Rippka, R., Deruelles, J., Waterbury, J.B., Herdman, M. and Stanier, R.Y., 1979, Generic assignment, strain histories and properties of pure cultures of cyanobacteria: Journal of General Microbiology, v. 111, p. 1-61.

Shuster J., Bolin, T., MacLean, L.C.W. and Southam, G., 2014, The effect of iron-oxidising bacteria on the stability of gold (I) thiosulphate complex: Chemical Geology, v. 376, p. 52-60.

Silverman, M.P. and Lundgren, D.G., 1959, Studies on the chemoautotrophic iron bacterium Ferrobacillus ferrooxidans. An improved medium and a harvesting procedure for securing high cell yields: Journal of Bacteriology, v. 77, p. 642-647.

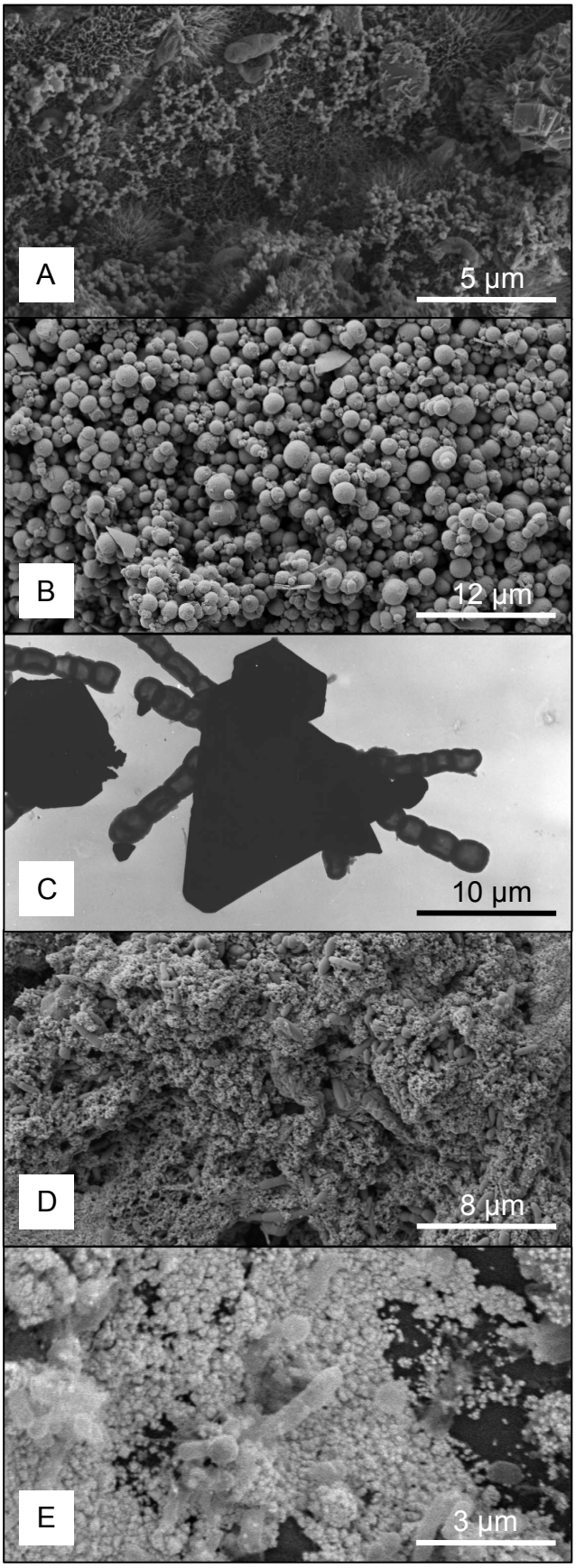

Figure DR1.1. Scanning and transmission electron micrographs of biogenic gold constituents added to the experimental system. A. A SEM micrograph of colloidal Au reduced from Au(I) thiosulfate by acidophilic IOB. B. A SEM micrograph of colloidal, gold sulfide resulting from reaction between Au(I) thiosulfate and ferric iron in solution (produced by actively metabolizing acidophilic IOB). C. A TEM micrograph of octahedral Au platelets associated with filamentous cyanobacteria. D. A SEM micrograph of colloidal Au reduced from Au(III) chloride by halophilic, SRB E. A SEM micrograph of colloidal Au reduced from Au(I) thiosulfate by SRB.

Figure DR2.1. A. A photograph of the experimental system. Elliptical and cylindrical Au grains occurred within the sand (circle) while smaller grains were trapped within the biofilm that was attached to the inner surface of the cylinder (arrow).

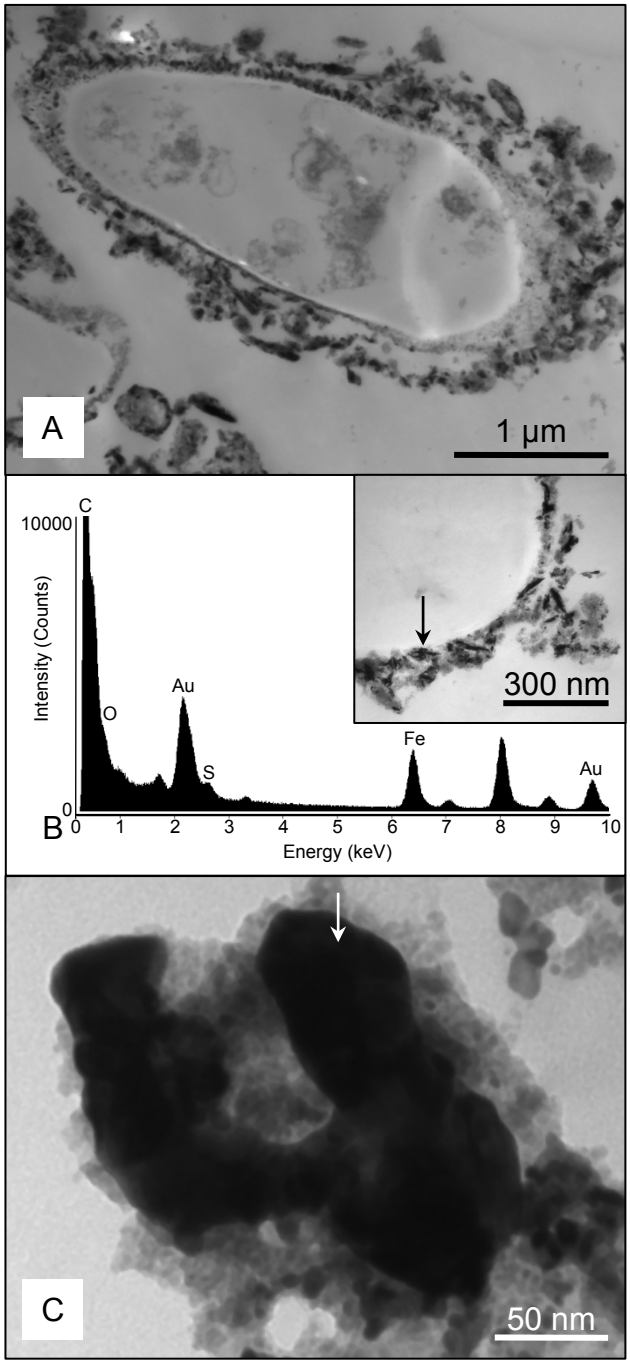

Figure DR2.2. A. An ultrathin section TEM micrograph of an extensively mineralized bacterial cell from within the biofilm. B. EDS analysis confirmed that mineralized cells were covered in Au particles (inset, arrow). The presence of Fe and S was also detected and was attributed to FeS(s) formed by the SRB consortium. Note that the unlabeled peak is Cu from the TEM grid. C. A high-resolution, whole mount TEM micrograph of the fluid phase demonstrated the presence of nanometer-size Au particles (arrow) that were suspended in solution.

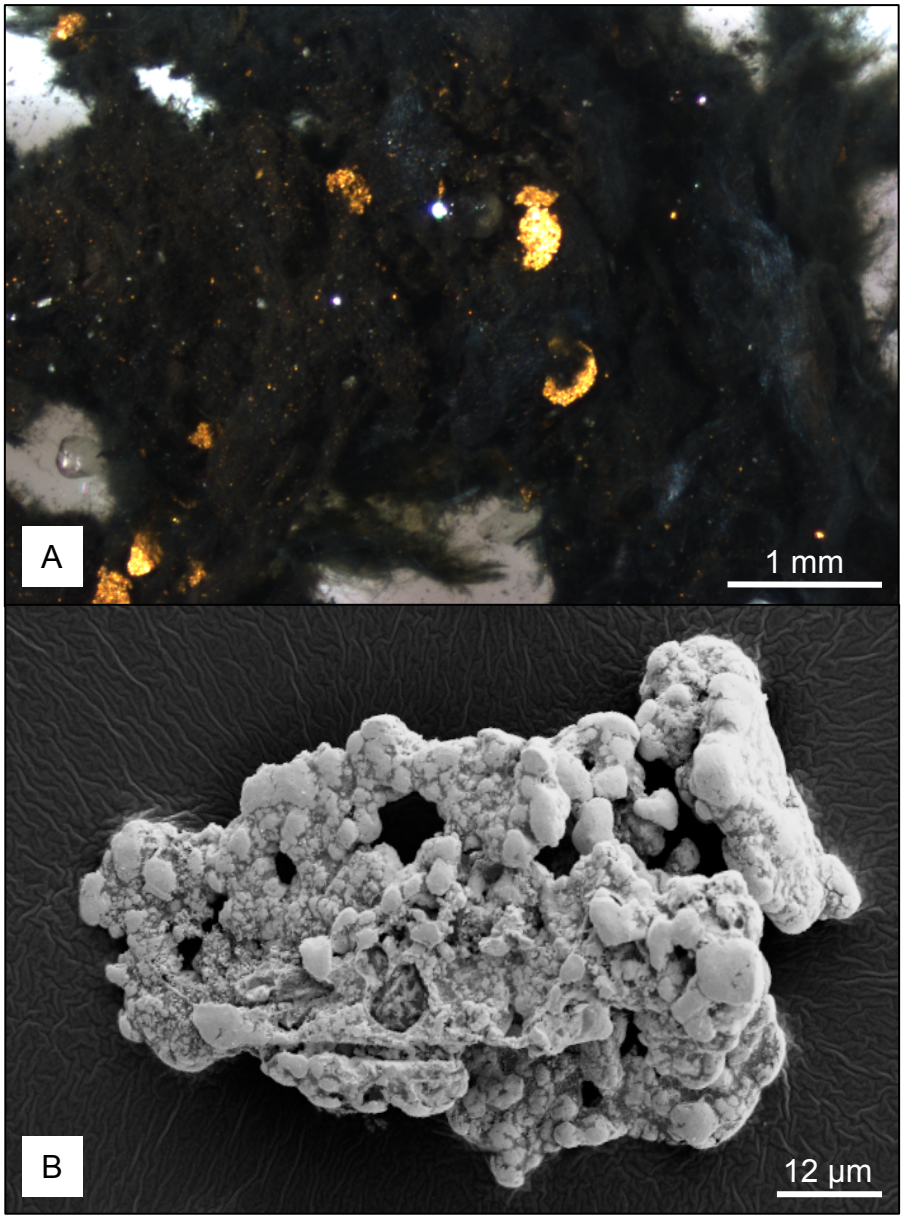

Figure DR2.3. A photograph demonstrating that sub-millimeter-scale Au particles were heterogeneously distributed throughout the biofilm. B. A backscatter SEM micrograph, representing the initial formation of micrometer-scale globular Au grains from the biofilm. These grain structures were comprised of aggregated nanometer- and micrometer-scale, secondary Au particles.

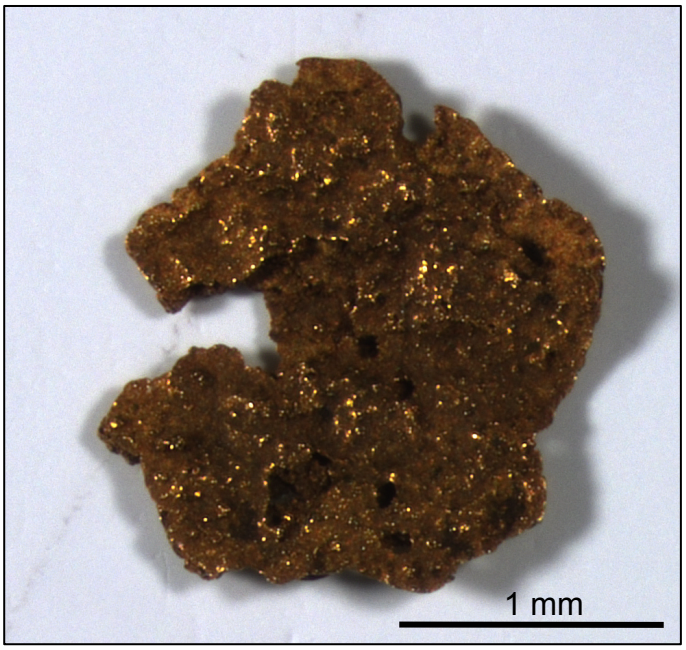

Figure DR2.4. A photograph of a representative elliptical, disk-shaped grain that occurred within the sediment of the experimental system.

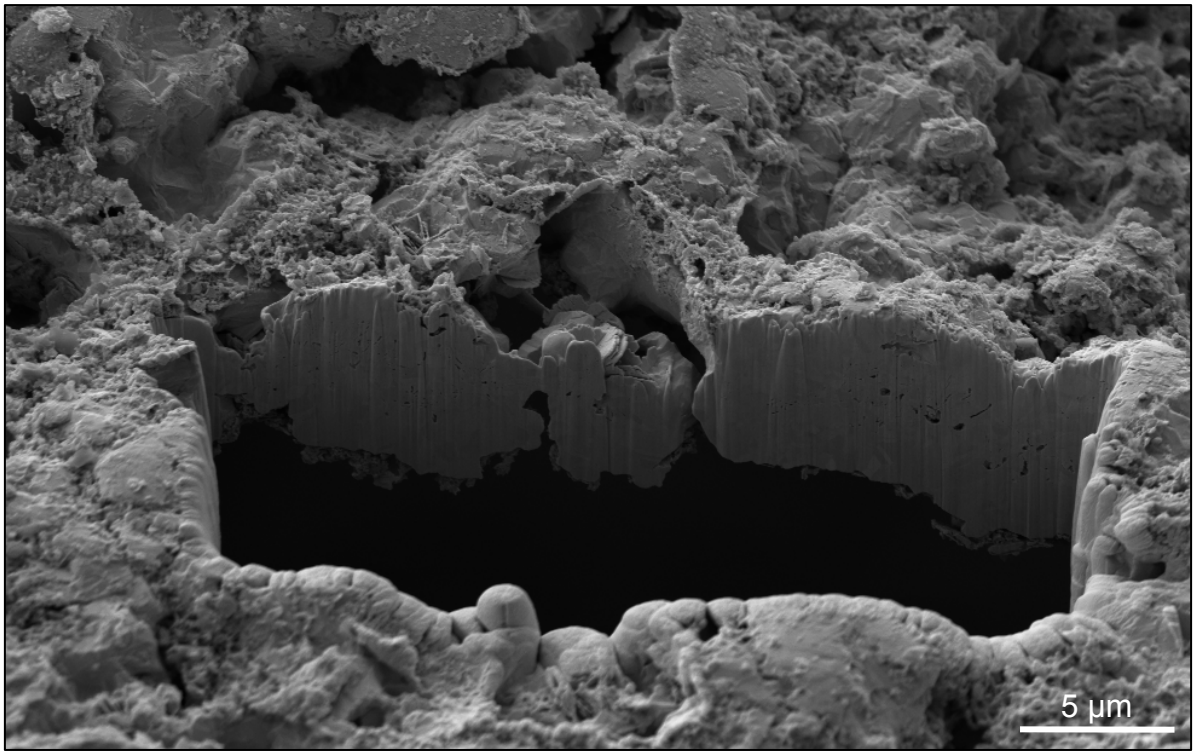

Figure DR2.5. A secondary electron SEM micrograph of a FIB-milled section on the surface of a representative cylindrical Au grain. The trough, cross-section demonstrated that the 'aggregation' of elliptical grains did not produce tightly compacted structures. Note the void (dark region) within the larger cylindrical grain.

Table DR2. Balance of Au fractions within the experimental system over time.

Week	Au_{Total} before sampling (mg)	$Au_{Soluble}$ (mg)	Au_{Solid} (Au_{Total} - $Au_{Soluble}$) (mg)	$Au_{Soluble}$ removed for analysis (mg)	Au_{Solid} removed for analysis (mg)*	Au remaining in bioreactor (mg)
0	525.8	57.0	468.8	1.14	--	524.6
2	524.6	62.7	461.9	1.28	--	523.4
4	523.4	61.5	461.9	1.23	10.15	512.0
6	512.0	55.4	456.6	1.13	--	510.9
8	510.9	53.0	457.9	1.06	12.13	497.7
10	497.7	49.1	448.6	0.98	--	496.8
12	496.8	47.7	449.0	0.97	12.91	482.8
14	482.8	48.0	434.8	0.96	208.31	481.8

*total mass of Au grains removed